**TELKOMNIKA Telecommunication, Computing, Electronics and Control**
Vol. 19, No. 2, April 2021, pp. 531~539
ISSN: 1693-6930, accredited First Grade by Kemenristekdikti, Decree No: 21/E/KPT/2018
DOI: 10.12928/TELKOMNIKA.v19i2.15914 

# New investigation of an E-mode metal-insulator-semiconductor AlInN/AlN/GaN HEMT with an Au-T-gate

**Asmae Babaya[1], Adil Saadi[2], Seddik Bri[3]**
[1,2]Control, Piloting and Supervision of Systems, Ecole Supèrieure d'Art et Mètiers,
Moulay Ismail University Meknes, Morocco
[3]Materials and instrumentation (MIM), High School of Technology, Moulay Ismail University Meknes, Morocco

**Article Info**

***Article history:***

Received Feb 24, 2020
Revised Jun 1, 2020
Accepted Jun 12, 2020

***Keywords:***

AlInN/AlN/GaN
E-mode
HEMT
T-gate
Threshold voltage

**ABSTRACT**

In a high electron mobility transistor (HEMT), the density of the two-dimensional electron gas (2DEG) channel is modulated by the application of a bias to a Schottky metal gate. These devices are depletion mode (D-mode), which means that a negative bias must be applied to the gate to deplete the electron channel and turn. The most challenging aspect in the present research activity on based-GaN devices is the development of a reliable way to achieve an enhancement-mode (E-mode) HEMT. Enhancement-mode GaN HEMTs would offer a simplified circuitry by eliminating the negative power supply. In this work, the aim is to investigate the different techniques which can influence the threshold voltage and shift it to a positive value. A novel E-mode metal-insulator-semiconductor (MIS) AlInN/GaN HEMT with an Au-T-gate has been investigated. The impacts of window-recess and deep-recess have been discussed, it was found that for dp=28 nm and wn=1.8 µm the threshold voltage achieves 0.7 V and the transconductance (Gm) peak value of 523 mS at Vgs=3.5 V. The drain current characteristic has been demonstrated.



***Corresponding Author:***

Asmae Babaya
Control, Piloting and Supervision of Systems, Ecole Supèrieure d'Art et Mètiers,
Moulay Ismail University
15290 ENSAM ،Meknes 50500, Morocco
Email: asmae.babaya@gmail.com

## 1. INTRODUCTION

The wireless communication industry has continued to witness exponential growth due to recent advances in modern electronics and semiconductor (SC) technologies [1]. Since 1960, silicon (Si) has been the most frequent SC for power electronics devices. However, today the continuous demand for higher current, voltage and power density capability, as well as the need of better energy efficiency to decrease the global energy consumption, is the main causes to bring in new semiconductor technologies in power electronics and to rise over the inherent limitations of Si-based devices [2, 3]. The wide bandgap SCs are the most promising technology for next-generation applications. Especially, the wide bandgap gallium nitride (GaN) has attracted attention as the highly bright material for electronic devices because of its excellent transport properties, high critical electric field, and thermal stability [4, 5]. It demonstrates high electron velocity (2.5x107 cm/s) and good electron mobility (>1500 $cm^2$/V.s). It has a high breakdown field (3 MV/cm) as well due to its wide bandgap (3.507 eV) [6, 7]. Over other highly demanded SCs such as Si and GaAs, GaN-based SCs offer five keys advantages, which are: high operating temperature, high critical electric field, high current densities, high-speed switching, and low on-resistances.

The development in GaN-based high HEMT technologies, radio-frequency power performance of conventional D-mode AlGaN/GaN has been given off and is approaching the limit of their material structures. The maximum output power of the device is limited by its maximum drain current and breakdown voltage. However, many power applications require the use of E-mode HEMT. The main challenge in the present research on GaN devices is developing an E-mode HEMT. The E-mode HEMT offers a simplified circuit; by eliminating the negative power supply. Several GaN HEMT structures have been proposed in the literature to meet the E-mode functionality [8-11]. To realize an E-mode HEMT and achieve a positive threshold voltage (Vth), many techniques have been presented: Increase the height of the Schottky barrier requires making a suitable choice of the material of the gate, the dielectric with high permittivity can be used [12, 13], but this technique does not have a significant impact on Vth [14]. Decrease the discontinuity band between GaN and barrier layer, in effect, this method decreases the density of 2DEG confined in the quantum well, which results in lower drain current. Fluorine ions ($F^-$) implantation under the gate has been used to achieve E-mode AlGaN/GaN HEMTs, all the ions should reside in the barrier layer, due to the channeling effect, and there is a high chance for ($F^-$) to be deeply implanted into the 2DEG channel, which degrades the electron mobility [15]. The easiest method, reduce the thickness of the barrier layer under the gate by using a recessed gate structure [16]. The recessed gate with a high permittivity combination can improve and increase the threshold voltage.

In this work, we present the results of a simulation of the DC characteristics of an E-modde GaN HEMT obtained using a recess etch technique. This paper is organized as follow: the device structure and the physical properties of the AlInN/AlN/GaN HEMT structure have been presented. To highlight the advantage of the gate structure, the influences of the deep recess-gate and window-recess etching on the threshold voltage and transconductance have been investigated. Then, the current drain characteristic has been demonstrated.

## 2. DEVICE STRUCTURE AND PHYSICAL PROPERTIES

### 2.1. Device structure

Figure 1 shows a cross-section of the epitaxial used to fabricate the device. The device under investigation was realized by TCAD-silvaco. The E-mode HEMT structure was grown on 1.5 µm sapphire as a substrate, which allows good thermal stability. The HEMT epitaxial begins with a 2 nm AlN nucleation layer allows to reduce strain, followed by an 800 nm undoped GaN layer, which maintains the rule of the channel. The optimized structure induced a 7 nm doped AlInN Barrier Layer, followed by a 30 nm high quality of dielectric layer within the gate recess; different properties of dielectric have been presented in Table 1. Finally, the electrodes have been deposited. Our choice of the gate material has been done after studied the resistivity and work function properties of several metals summarized in Table 2. The source-drain length is 8 µm; the source-gate length is 2 µm [17].

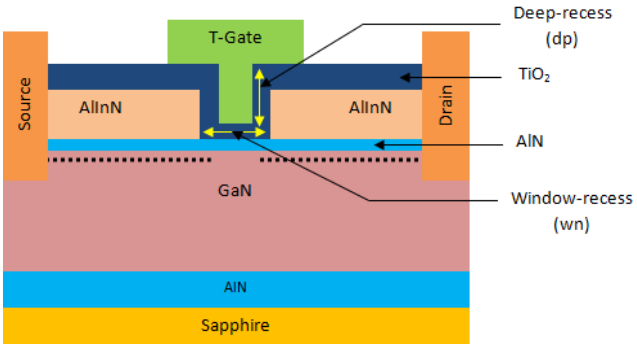


Figure1. Cross-section of the AlInN/AlN/GaN MIS-HEMT with a recessed-gate

Table1. Properties of high-K dielectric materiel [18, 19]

| Material | ε (F/m) | C (J/K) | K(W/(m.k) | Gap (Ev) | Ec (eV) | Ev (eV) |
|---|---|---|---|---|---|---|
| SiO2 | 3.9 | 3.066 | 0.014 | 9 | 3.5 | 4.4 |
| SiN | 7.5 | 0.585 | 0.185 | - | - | - |
| Al2O3 | 9.3 | 3.14 | 0.29 | 8.8 | 3 | 4.7 |
| HfO2 | 22 | - | - | 5.8 | 1.4 | 1.3 |
| TaO5 | 26 | - | - | - | - | - |
| TiO2 | 80 | - | - | 3.5 | 1.1 | 1.3 |

Table 2. Resistivity and temperature coefficient of metals [20]

| Material | $\sigma(\mu\Omega.cm)$ | $R(\mu\Omega.cmK^{-1})$ | W(eV) |
|---|---|---|---|
| Gold | 2.35 | 0.004 | 5.93 |
| Silver | 1.59 | 0.0041 | - |
| Tin | 11.0 | 0.0047 | 4.53 |
| Platinum | 10.6 | 0.003927 | 5.65 |
| Nickel | 6.84 | 0.0069 | 5.04 |

### 2.2. Physical properties

The AlInN/AlN/GaN HEMTs is characterized by channel formation [21]. High levels of polarization at the interface of AlInN/AlN/GaN heterojunction induce a polarization sheet charges σ in the high bandgap of AlInN, which causes the accumulation of attracted mobile carriers, electrons in the case of a positive sheet charge σ, confined in a quantum well along the heterojunction. This electron accumulation induced by polarization is called a 2DEG. The confined electrons present a very high mobility 1360 $cm^2$/V.s, which is main characteristic of HEMTs. Therefore, the polarization modeling is critical for GaN-based devices. The induced sheet charge σ created at the interface between the AlInN layer and the GaN layer can be written as the function of spontaneous and piezoelectric polarization across the heterostructure interface, it is given by the following equation [22]:

$$\sigma = \left(P_{SP-Al_{1-x}In_xN} + P_{PE-Al_{1-x}In_xN}\right) - P_{SP-GaN} \quad (1)$$

The primary parameter to enhance the performance of AlInN/AlN/GaN HEMTs is the concentration of 2DEG (ns) [21]. Understanding the physical phenomena governing the operation of the HEMT and the formation of a 2DEG requires solving the Schrödinger's and Poisson's equation [23]. The solution of Schrodinger's equation gives a quantized description of the density of states in the presence of quantum mechanical confining potential variations. In situations where there is strong quantum confinement in the SC, Atlas can include charge quantization effects. To do this, use the Schrodinger-Poisson solver. Once the carrier concentration is calculated using (2), it is substituted into the charge part of Poisson's Equation. The potential derived from the solution of Poisson's equation is substituted back into Schrodinger's equation. This solution process (alternating between Schrodinger's and poisson's equations) continues until convergence and a self-consistent solution of Schrodinger's and Poisson's equations are reached. A default predictor-corrector scheme is used to avoid instability and oscillations of poisson convergence. In obtaining self-consistent solutions for the Schrodinger's Equation, an assumption is made about the location of the electron or hole quasi-fermi level. Normally, atlas tries to set the quasi-fermi to that of a contact attached to the region where the solution is obtained [19].

$$\begin{cases} n(x,y) = \frac{2K_BT}{\pi h^2}\sum_v \sqrt{m_x^v(x,y)m_z^v(x,y)}\sum_v^\infty |\psi_{iv}(x,y)|^2 \, ln\left[1 + exp\left(-\frac{E_{iv}-E_F}{K_BT}\right)\right] \\ n(x,y) = \frac{2K_BT}{\pi h^2}\sum_v \sqrt{m_z^v(x,y)}\sum_v^\infty |\psi_{iv}(x,y)|^2 \, F_{-1/2}\left(-\frac{E_{iv}-E_F}{K_BT}\right) \end{cases} \quad (2)$$

To maintain self-consistency, we need to take into account that electrons are being emitted or captured by the donor and acceptor-like traps. Therefore, the concentration of carriers will be affected. This is accounted for by modifying the recombination rate in the carrier continuity equations. Phonon transitions occur in the presence of a trap (or defect) within the forbidden gap of the SC. This is essentially a two steps process, the theory of which was first derived by Shockley and Read [24] and then by Hall [25]. The Shockley-Read-Hall recombination is modeled as follows:

$$R_{SRH} = \frac{pn - n_{ie}^2}{\tau_p[n + n_{ie}\,exp(E_{trap}/KT_L)] + \tau_n[p + n_{ie}\,exp(-E_{trap}/KT_L)]} \quad (3)$$

where $E_{TRAP}$ is the difference between the trap energy level and the intrinsic Fermi level, $T_L$ is the lattice temperature in degrees Kelvin, $\tau_n$ and $\tau_p$ are the electron and hole lifetimes.

We have taken into account the low and the high field mobility to consider various types of scattering mechanisms during the two-dimensional numerical calculation. Following the work of Albrecht, the low field mobility, as a function of doping and lattice temperature, can be given by following equation and the default parameter values for the Albercht Model are summarized in Table 3 [26]:

$$\frac{1}{\mu(N,T_L)}=\frac{AN.ALBRCT.N}{N0N.ALBRCT}\left(\frac{T_L}{T0N.ALBRCT}\right)^{-3/2}*ln\left[1+3\left(\frac{T_L}{T0N.ALBRCT}\right)^{2}\left(\frac{N}{T0N.ALBRCT}\right)^{-3/2}\right]$$
$$+BN.ALBRCT\left(\frac{T_L}{T0N.ALBRCT}\right)^{3/2}+\frac{CN.ALBRCT}{exp(T1N.ALBRCT/T_L)^{-1}} \quad (4)$$

Table 3.Default parameter values for the Albrecht model [26]

| Parameter | Default | Units |
|---|---|---|
| AN.ALBRCT | 2,61.10-4 | V.s/cm2 |
| BN.ALBRCT | 2,9.10-4 | V.s/cm2 |
| CN.ALBRCT | 170.10-4 | V.s/cm2 |
| N0N.ALBRCT | 1.1017 | cm-3 |
| T0N.ALBRCT | 300 | K |
| T0N.ALBRCT | 1065 | K |

The nitride specific field-dependent mobility model is based on a fit to Monte Carlo data for bulk nitride, which is described in the following equation and Table 4 presents the values of default nitride field dependent mobility mode parameter [27]:

$$\mu(E)=\frac{\mu(N,T)+v_{sat}E^{(N_1-1)}/E_C{}^{N_1}}{1+A_N(E/E_c)^{N_2}+(E/E_c)^{N_1}} \quad (5)$$

The AlInN/GaN heterojunction is used to take advantage of the 2DEG density. The total charge accumulated in the potential well and the threshold voltage are given simply by following equations [21]:

$$n_s=\frac{2q\varepsilon_{AlInN}m_e^*}{2dq^2m_e^*+\varepsilon_{Al\,ln\,N}\pi\hbar^2}\left(V_{gs}+V_{th}\right) \quad (6)$$

$$V_{Th}=\varphi_b-\Delta E_c-\sigma d_{AlInN}/\varepsilon_{AlInN} \quad (7)$$

$$\begin{cases}\Delta E_c=0.7\left[E_g(x)-E_g(0)\right]\\ E_g=xE_g(InN)+(1-x)E_g(InN)\end{cases} \quad (8)$$

Table 4. Default nitride field dependent mobility model parameter values [27]

| Material | vsat(cm/s) | Ec(kV/cm) | N1 | N2 | AN |
|---|---|---|---|---|---|
| GaN | 1,906.107 | 220,8936 | 7,2044 | 0.7857 | 6.1973 |
| InN | 1,359.107 | 52,4242 | 3,8501 | 0,6078 | 2,2623 |
| AlN | 2,167.107 | 447,0339 | 17,3681 | 0.8554 | 8.7253 |

To develop a E-mode HEMT, as we can see in (7), several techniques can shift the threshold voltage to positive value. First, increasing the height of schottky barrier, schottky gate metals with higher work function can be used to increase the schottky barrier height. However, the choice of appropriate gate materiel is limited and its impact is not significant. Second, decrease the discontinuity band by reducing the aluminum and indium molar fraction on the barrier layer in (8) [28]. However, the objective of using lattice matched AlInN/GaN will not be achieved and the 2DEG density will reduce which impact also the drain current. Third, reduce the barrier thickness under the gate; this will be achieved by using T-gate and varying the recess-window and recess-deep. the 2DEG can be completely depleted at zero gate bias and E-mode HEMTs are formed, with a deep-enough gate-recess etching. The disadvantage of this technique is that the drain current drops too. Fourth, Fluorine ions ($F^-$) implantation under the gate is a smart option and has been used to achieve normally off AlInN/GaN HEMTs. Incorporated Fluorine ions act as immobile negative charges that can deplete the 2DEG and positively shift Vth. Ideally, all the $F^-$ ions should reside in the AlInN layer. However, due to the channeling effect for the $F^-$ ions in GaN lattice structure, as well as the non-uniformity in $F^-$ion energy distribution, there is a high chance for some $F^-$ ions to be deeply implanted into the 2DEG channel, which degrade the electron mobility by impurity scattering. Generally, when converting from D-mode to E-mode, $I_{DS,\,max}$ drops by more than 40% [11].

## 3. RESULTS AND DISCUSSION

We present the results of a simulation of the DC characteristics of a normally-off GaN HEMT obtained using a recess etch gate technique. Figure 2 illustrates the polarization charge induced at the interface by spontaneous and piezoelectric polarizations; the addition of a thinner AlN layer allows increasing the value of the polarization charge at the interface AlN/AlInN. The AlInN/AlN/GaN HEMT achieves a very high value of the 2DEG, which is cannot only be accounted to the presence of high polarization. The large band discontinuity between AlInN and GaN is responsible too. Figure 3 (a) shows the conduction band energy for the AlInN/AlN/GaN heterojunction. The discontinuity in the band gap between the different layers forms a quantum well at the interface, which is illustrated by Figure 3 (b) the present of a thinner AlN layer contributes to improve the confinement of the 2DEG at the quantum well.

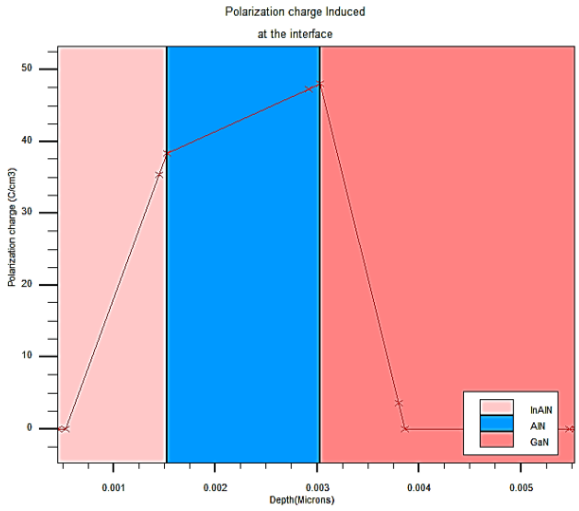


Figure 2. Polarization charge induced at the AlInN/AlN/GaN

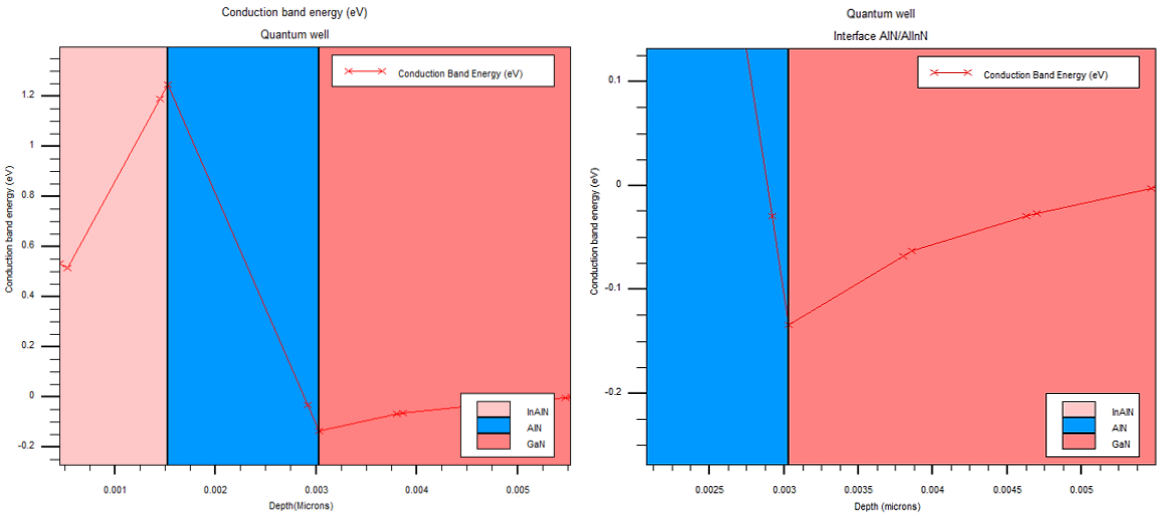


(a) (b)

Figure 3. (a) Conduction band energy at the interface of the heterojunction, (b) quantum well

In order to highlight the impact of deep-recess gate etch, the window-recess has been fixed at wn=1.7µm and the deep-recess has been varied from 24 nm to 28 nm by a step of 2 nm. Figure 4. displays the transfer function characteristics and transconductance of the AlInN/AlN/GaN HEMT at $V_{ds}$=10 V. It was found that the threshold voltage shifted to a positive value for $d_p$=28 nm, with a threshold voltage between +0.5 V et 1 V as extracted from the linear extrapolation of the I-V curve. The peak extrinsic transconductance of the studied device achieves a high value with a deeper etching gate, it was measured to be 523 mS at $V_{gs}$=3.5 V.

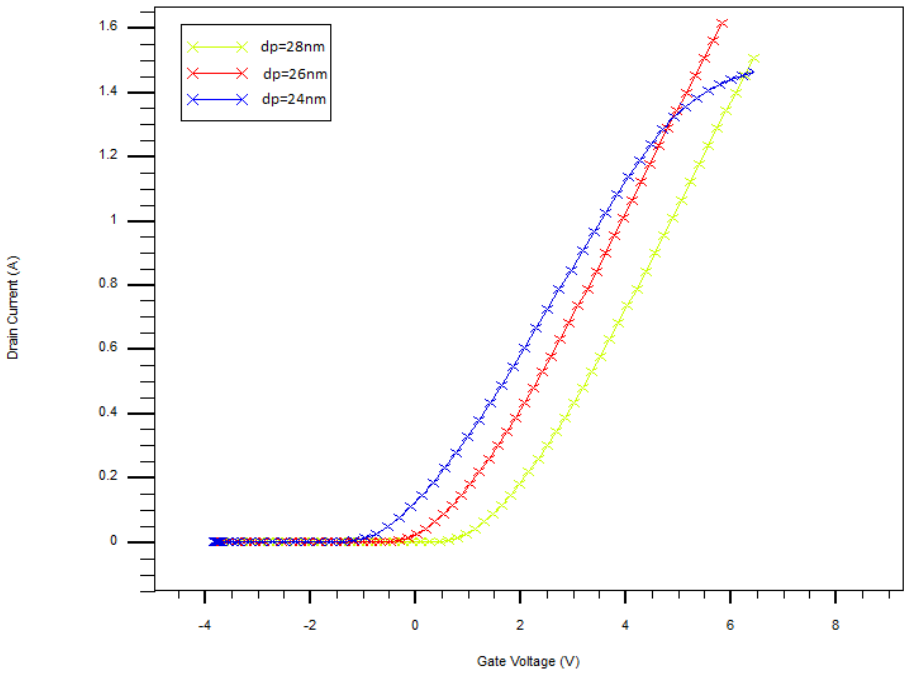


(a)

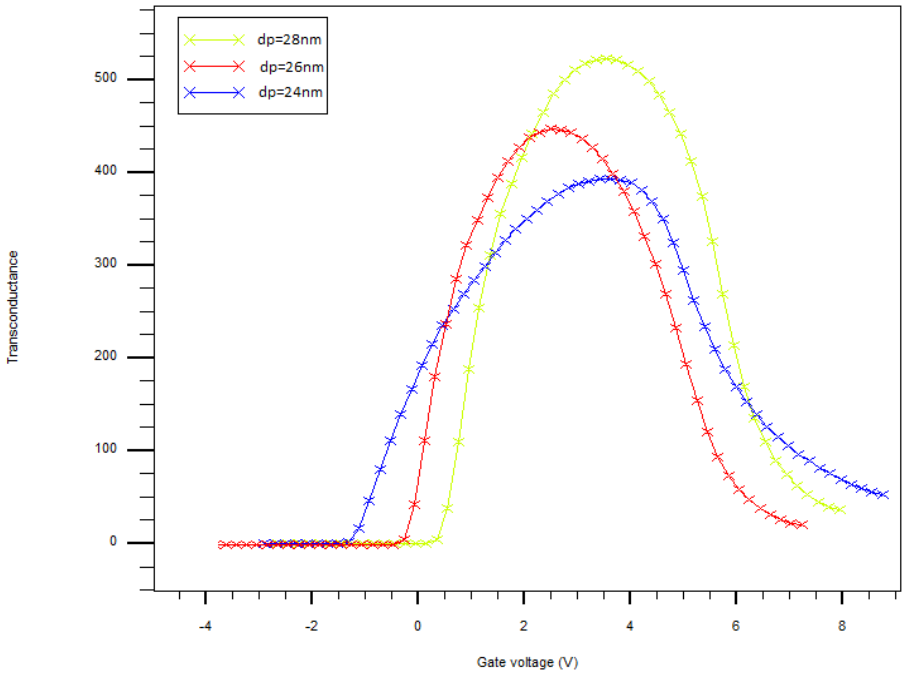


(b)

Figure 4. (a) Transfer function, (b) Transconductance for $w_n$=1.7µm and versus values of the deep-recess gate (dp)

According to the previous result, the deep-recess has been fixed at dp=28nm and the window-recess gate etch has been varied from 1.6 µm to 1.8 µm by a step of 0.1 µm. Figure 5 shows the transfer function and the transconductance of the AlInN/AlN/GaN HEMT at $V_{ds}$=10 V. This result shows perfectly that reducing the barrier layer under the gate leads to a positive value of the threshold voltage as has been presented in the bellow section. On the other hand, it was seen that the values of transconductance and the curves of Vg-Id decrease with the window-recess. The drain current characteristic is illustrated in Figure 6 the maximum saturation

current density for this device was almost 1A at Vgs=+4 V which is higher compared to the value reported in [17]. As has been shown the drain current is almost null for Vgs=0 V, which means that the proposed structure allows obtaining a normally-off AlInN/AlN/GaN HEMT and presents an excellent potential for power electronic applications.

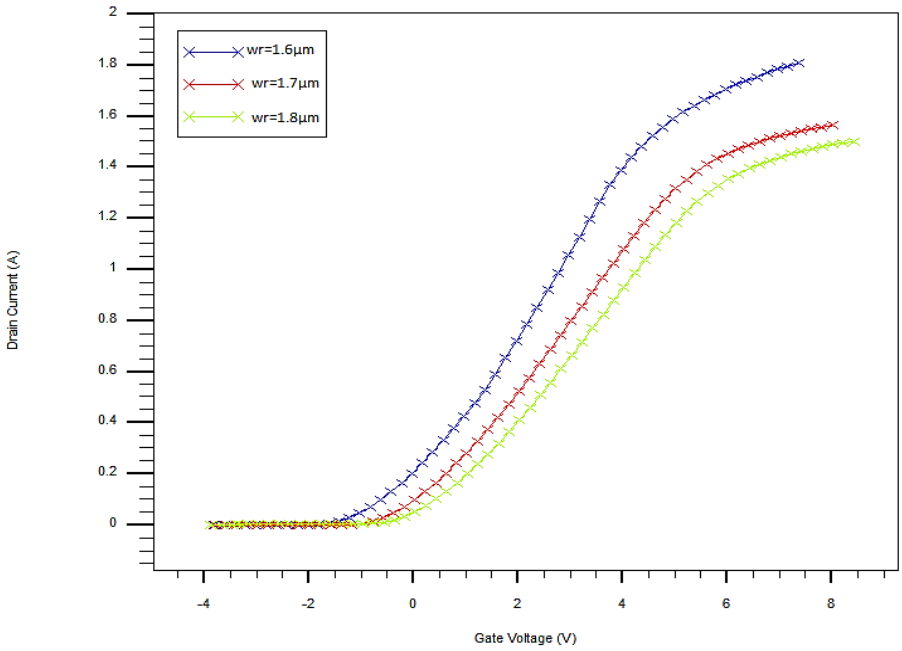


(a)

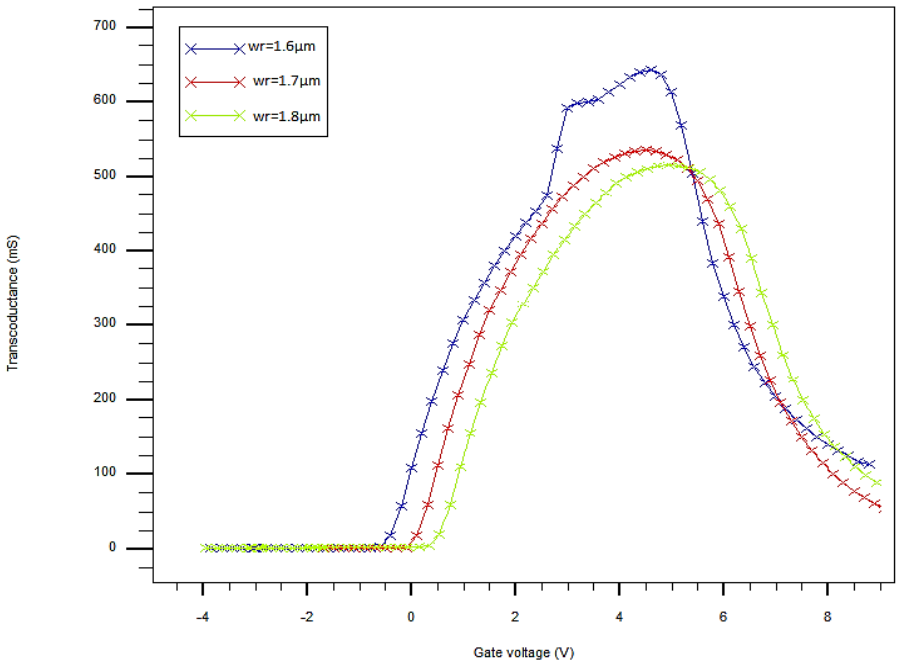


(b)

Figure 5. (a) Transfer function (b) Transconductance for dp=28 nm and different values of the window-recess gate (wn)

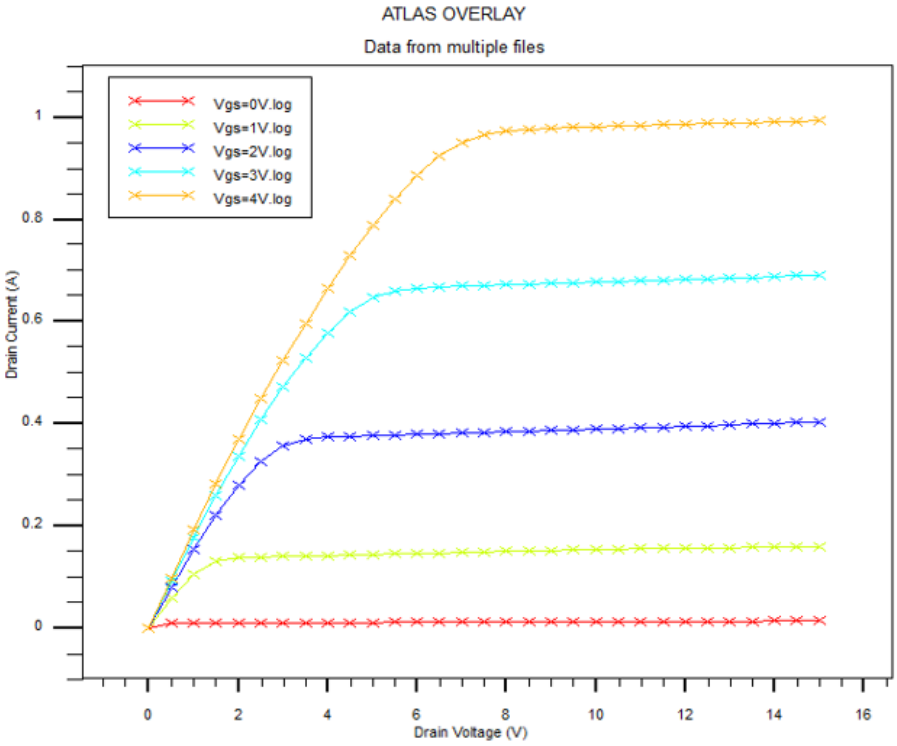


Figure 6. Ids-Vds characteristic for wn=1.8 µm and dp=28 nm

## 4. CONCLUSION

In this work, a novel E-mode metal-insulator-Semiconductor AlInN/AlN/GaN HEMT has been investigated. The influence of the deep-recess and window recess gate etch on the threshold voltage has been studied. The optimal values to shift the threshold voltage to a positive value of 0.7 V are wn=1.8 µm and pd=28 nm. The transconductance peak value Gm=523 mS at Vgs=+3.5 V. The proposed structure of AlInN/AlN/GaN HEMT allows obtaining a drain current characteristic null for Vgs=0 V.

## REFERENCES

[1] O. Ojewande, C. Ndujiuba, A. A. Adelakun, S. I. Popoola, and A. A. Atayero "Negative resistance amplifier circuit using GaAsFET modelled single MESFET," *TELKOMNIKA Telecommunication, Computing, Electronics and Control,* vol. 18, no. 1, pp. 179-190, February2020.

[2] F. Roccaforte, G. Greco, P. Fiorenza, and F. Iucolano, "An Overview of Normally-Off GaN-Based High Electron Mobility Transistors,"*Materials*, vol. 12, no. 10, pp. 1-18, 2019.

[3] P. Nakkala, "Pulsed I-V and RF characterization and modeling of AIGaN HEMTs and Graphene FETs," Thesis, Electronics. Université de Limoges, 2015.

[4] U. K. Mishra, L. Shen, T. E. Kazior, and Y. F. Wu, "GaN-based RF power devices and amplifiers," *Proc. IEEE*, vol. 96, no. 2, Feb. 2008, pp. 287-305.

[5] Y. Tang, *et al.,* "Ultrahigh-speed GaN high-electron-mobility transistors with fT/fmax of 454/444 GHz," *IEEE Electron Device Letter*, vol. 36, no. 6, pp. 549-551, Jun 2015.

[6] H. Frederick *et al.*, "RF and Microwave Power Amplifier and Transmitter Technologies," *High Frequency Electronics,* pp. 22-54, May 2003.

[7] H. Saidi, S. Ridene, H. Bouchriha, "Hole intersubband transitions in wurtzite and zinc-blende strained AlGaN/GaN quantum wells and its interband interaction dependence," *International Journal of Modern Physics B,* vol. 29, pp. 1550054-1-18, 2015.

[8] G. Kurt, *et al*., "Investigation of a Hybrid Approach for Normally-Off GaN HEMTs Using Fluorine Treatment and Recess Etch Techniques," *IEEE Journal of Electron device society*, vol. 7, pp. 351-357, 2019.

[9] Z. E. Touati, Z. Hamaizia, Z. Messai, "Design and analysis of 10 nm T-gate enhancement-mode MOS-HEMT for high power microwave applications," *Journal of Science: Advanced Materials and Devices,* vol. 4, no. 1, pp. 180-187, 2019.

[10] P. Murugapandiyan, S. Ravimaran, J. William, and K. M. Sundaram, "Design and Analysis of 30 nm T-Gate InAlN/GaN HEMT with AlGaN back-barrier for High power Microwave Applications," *Superlattices and Microstructures,* vol. 111, pp. 1050-1057,2017.

[11] M-H. Mi, *et al.*, "90 nm gate length enhancement-mode AlGaN/GaN HEMTs with plasma oxidation technology for high-frequency application," *Applied Physics Letter*, vol. 111, no. 17, 173502, 2017.
[12] M. A. Ismail, K. M. M. Zaini, and M. I. Syono, "Graphene field-effect transistor simulation with TCAD on top-gate dielectric influences," *TELKOMNIKA Telecommunication, Computing, Electronics and Control,* vol. 17, no. 4, pp.1845-1852, August 2019.
[13] A. M. Dinar, A. S. Zain, F. Salehuddin, K. M. Mowafak, L. A. Mothana, and M. K. Abdulhameed, "Performance analysis of high-k materials as stern layer in ion-sensitive field effect transistor using commercial TCAD," *TELKOMNIKA Telecommunication, Computing, Electronics and Control,* vol. 17, no. 6, pp. 2867-2876, 2019.
[14] M. Sultana. "Technology Development and Characterization of AIInN/GaN HEMTs for High Power Application," Doctoral dissertation, Electric Engineering, University of South Carolina,2015.
[15] Y. Cai, Y. Zhou, K. M. Lau, and K. J. Chen, "Control of Threshold Voltage of AlGaN/GaN HEMTs by Fluoride-Based Plasma Treatment: From Depletion Mode to Enhancement Mode," *IEEE Transactions on Electron Devices,* vol. 53, no. 9, pp. 2207- 2215, 2006.
[16] W. Saito, Y. Takada, M. Kuraguchi, K. Tsuda and I. Omura, "Recessed-gate structure approach toward normally off high-Voltage AlGaN/GaN HEMT for power electronics applications," *IEEE Transactions on Electron Devices*, vol. 53, no. 2, pp. 356-362, Feb. 2006.
[17] M. Daniel, *et al.*, "Enhancement-Mode Insulating-Gate AlInN/AlN/GaN Heterostructure Field-Effect Transistors with Threshold Voltage in Excess of +1.5 V," *Applied Physics Express*, vol. 4, no. 11, 2011.
[18] Y. Yeo, T. King, and C. Hu, "Metal-dielectric Band Alignment and its Implications for Metal Gate complementary Metal Oxide Semiconductor Technology," *J. Appl. Phys.,* vol. 92, no. 12, pp. 7266-7271, Dec. 15, 2002.
[19] Silvaco int. Atlas User's Manual Device Simulation Software: Santa Clara, CA 95054, 2016. [Online]. Available at: www.silvaco.com
[20] W. M. Haynes, Ed. "CRC Handbook of Chemistry and Physics," *CRC Press*, 2014-2015.
[21] A. Babaya, S. Bri, A. Saadi, "Influence of AlN Interlayer on the Performance of InAIN/GaN HEMT,"*in proc. InternationalSymposium on Advanced Electrical and Comuunication Technologies,* Rabat, 2018, pp. 1-4.
[22] O. Ambacher, *et al.,* "Two-dimensional electron gases induced by spontaneous and piezoelectricpolarization charges in N- and Ga-face AlGaN/GaN heterostructures," *Journal of Applied Physics,* vol. 85, no. 6, pp. 3222-3233, 1999.
[23] A. Babaya, S. Bri, A. Saadi, "Analytic Estimation of Two-Dimensional Electron Gas Density and Current-Voltage Characteristic in AlGaN/GaN HEMT's," *International Journal of Electrical and Computer Engineering,* vol. 81, no. 2, pp. 954-962, April 2018.
[24] W. Shockley, and W.T. Read, "Statistics of the Recombination of Holes and Electrons," *Phys. Rev*., vol. 87, pp. 835-842, 1952.
[25] R. N. Hall, "Electron Hole Recombination in Germanium," *Phys. Rev.,* vol. 87, pp. 387, 1952.
[26] J. D. Albrecht, R. P. Wang, P. P. Ruden, M. Farahmand, and K. F. Brennan, "Electron transport characteristics of GaN for high temperature device modeling," *J. Appl. Phys,* Vol. 83, pp. 4777-4781, 1998.
[27] M. Farahmand, *et. al.,* "Monte Carlo Simulation of Electron Transport in the III-Nitride Wurtzite Phase Materials System: Binaries and Terniaries," *IEEE Trans. Electron Devices*, vol. 48, no. 3, pp. 535-542, 2001.
[28] J. Piprek, "Semiconductor Optoelectronic Devices: Introduction to Physics and Simulation," *UCSB: Academic Press: 22,* 2003.